

EXPERIMENTAL RESEARCH OF FORCE/PRESSURE SENSOR STATIC AND DYNAMIC ACCURACY AND REPEATABILITY

Nikita Edgar Sitiajev¹, Vaiva Treciokaite¹, Ernestas Šutinys¹

¹ Department of Mechatronic, Robotics and Digital Manufacturing, Vilnius Gediminas Technical University, Vilnius

nikita-edgar.sitiajev@stud.vgtu.lt; vaiva.terciokaite@stud.vgtu.lt; ernestas.sutinys@vilniustech.lt

Design of testing stand

During the research, the velostat® film was placed between two conductive copper electrodes which allowed to measure the resistance of the material in respect of time and evaluate sensors' dynamic response.

Dynamic load acting on the sensor's upper surface was created using a motor carrying an eccentric load (Fig. 1.). By changing the mass and adjusting the loading fixture offset from motor shaft different magnitude mechanical loads were exerted. The loading frequency was controlled by the stepper motor's varying rotation speed.

From the Fig. 1 you can observe a velostat® film (1) being placed between two conductive strips (2), to connect it to measuring device, placed between a lower (3) and upper (4) plates to hold it in place. The upper plate is represented transparent, in order to show the interconnection between the elements. The upper plate is firmly connected to the motor (5), which is going to create an eccentric load for force-sensitive material. On the shaft of the motor a pulley (6) with slots is mounted, in order to allow attachment and adjustment of different weights making testing device more versatile also an accelerometer (7) is joined with the upper plate to monitor the magnitude of excited force.

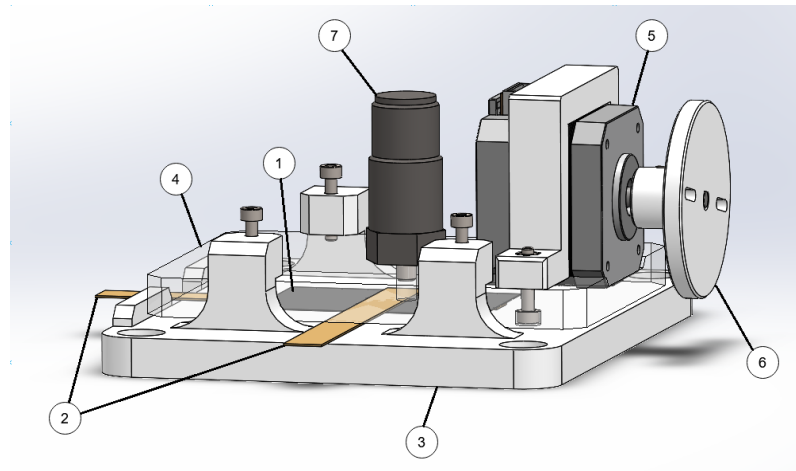


Fig. 1. Testing device scheme: 1 - Velostat® film, 2 - conductive strip, 3 - bottom plate, 4 - upper plate, 5 - electric motor, 6 - pulley, 7 - accelerometer

From Fig. 2 working principle of whole system can be noted. For testing device (4) actuation stepper motor requires power supply and motor control for this reason stepper motor is connected to motor drive circuit (3). Motor drive obtains stable VDC current from adjustable ADC (2), which serves as power supply. Laptop (1) through microcontroller is connected to stepper motor drive allowing to control stepper motor rotational velocity. In order to retrieve data from testing device two accelerometers and velostat® is routed to data acquisition unit (6). One of accelerometers is fixed on the upper plate of testing device and another one is screwed into magnet and placed on vice, in which testing device is firmly fastened. Velostat® film from testing device through copper contacts is connected first to resistance to voltage value converter (5) then to data acquisition unit, from where all values are loaded into laptop and sensor value correlation to time is stored.

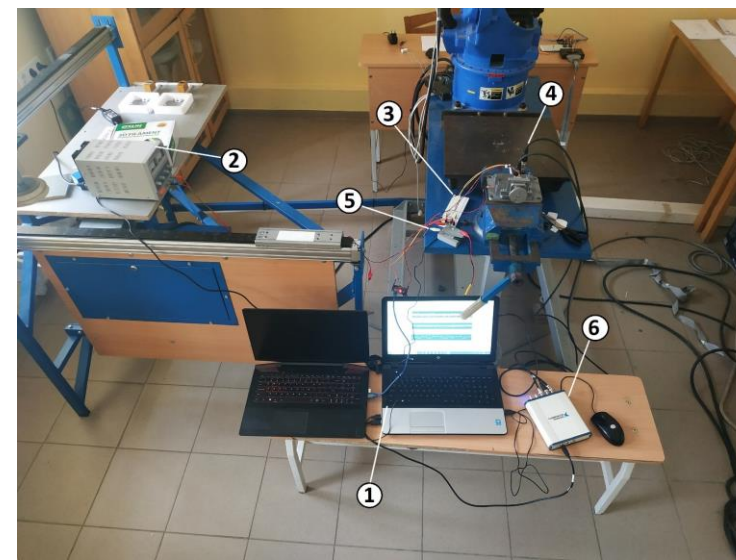


Fig. 2 General view of testing stand: 1 - Laptop, 2 - DC power supply, 3 - Stepper motor drive circuit, 4 - testing device, 5 - Resistance to voltage converter, 6 - Data acquisition device.

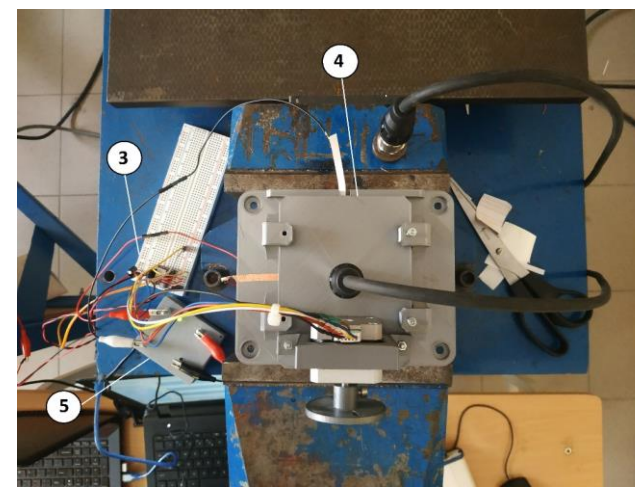


Fig. 3 Magnified part of general view: 3 - Stepper motor drive circuit, 4 - testing device, 5 - Resistance to voltage converter.

When the experiment is carried out, data is obtained and saved on the memory device. Correlation between frequency and amplitude of applied dynamic load and change in resistance of velostat® defines how precisely sensor can react to varying load. Obtained data allows defining the sensor's main dynamic characteristics such as response time and bandwidth.

After result evaluation, precise velostat® reaction is established, promoting the further implementation of force-sensitive material into "soft robotics" applications.

Equipment

During static and dynamic pressure / force sensitive material, velostat®, experimental research following equipment was used.

Accelerometer: IMI Model 603C01
Data acquisition unit: NI USB-4432
Stepper motor: NEMA 17 SM-42BYG011-25
Stepper motor drive: DRV8825
Microcontroller: Arduino UNO
VDC power supply: Mastech HY3005C

All custom parts for testing device were designed and 3D printed from PETG plastic and assembled using common metric fasteners.

Acknowledgement

This project has received funding from the European Social Fund (project No 09.3.3.-LMT-K-712-22-0328) under a grant agreement with the Research Council of Lithuania (LMTLT).

Introduction

The progress observed in 'soft robotics' brought some promising research in flexible tactile, pressure and force sensors, which can be based on polymeric composite materials. Therefore, in this paper, we intend to evaluate the characteristics of a force-sensitive material – polyethylene-carbon composite (Velostat®) by implementing this material into the design of the flexible tactile sensor [1].

It can be used for various purposes, especially in the design of flexible sensors, which are highly demanded for mechatronics and biomedical application. The typical application field of flexible piezo resistive sensors covers the evaluation of pressure or applied normal force in non-stiff objects, such as normal stress in various materials [2], normal soil stresses [3], normal stresses in other objects with high lateral deformation [4, 5]. Flexible piezoresistive sensors can be applied in robotics [6-8], wearable sensors [9] and human-machine interaction devices [10]. However, the implementation of a piezoresistive sensors in mechatronic and robotic systems is still limited by the lack of reliable materials, which have stable characteristics [1, 11].

The main problem is an insufficiency of research of Velostat®, in order to successfully predict its reaction to particular mechanical irritation and therefore implement it as a reliable sensor in a mechatronic system.

Research object

Velostat® is a composite polymer material consisting of carbon-impregnated polyethylene. Entrapped carbon powder turns initially dielectric polyethylene into electrically conducting composite material which belongs to the group of piezoresistive materials. Simply speaking by applying force or pressure on this material, its resistance is changed.

In Table 1 known physical properties of Velostat® are presented.

Table 1. Velostat® physical properties [12]

Thickness, mm	0.1 - 0.2
Density, kg/m ³	1 190
Volume resistivity, Ω·cm	<500
Surface resistivity, Ω/m ²	<31 000
Temperature Limits, °	-45 - +65

In order to consider Velostat® as a material suitable for tactile sensor implementation its advantages and disadvantages should be examined.

The most significant advantages of resistive sensors comparing them to the sensors of other types are low manufacturing cost, simplicity of interfacing circuits and data acquisition process. The possibility to adjust sensor measurement range for required load within varying its geometric size and larger surface area allows measuring higher distributed load. Implementations of Velostat® material as a sensitive layer of the sensors in applicable devices have been reviewed in many studies. [...] Recently, Velostat® - based structures were implemented for various applications, but the evaluation of Velostat® electrical and mechanical characteristics is still insufficient [1].

Advantages:

- Flexible range of dimensions
- Mechanical and chemical stability
- Relatively low price

These limiting factors result in poor accuracy, repeatability, and ability to be easily replaced, which makes these sensors unsuitable for precise, repeatable and reliable pressure or force measurements. [...] Overcoming these problems will increase the application area of Velostat®, especially towards the application of this composite polymer in high-performance sensors [1].

Disadvantages:

- Aging causes change of electrical properties
- Nonlinear
- Significant hysteresis
- Non-homogenous structure
- Multidirectional conductivity

Therefore, detailed research of its characteristics is required, and algorithms to compensate their uncertainties needs to be elaborated and implemented.

Experimental research

Methodology

For velostat® pressure / force sensitivity evaluation static and dynamic tests were carried out. A single layer of 23.4 x 18.6 mm velostat® film was taken and with combination of copper conducting strips fixed in the centre of testing device's bottom plate.

In order to find out how velostat® reacts on constant loading static test was introduced. Different size weights were placed in the centre of upper testing device plate as shown in the Fig. 4. Totally 6 different weight tests were conducted, following with 0 g, 20 g, 50 g, 100 g, 150 g and 170 g weights. Each loading test lasted for 20 seconds.



Fig. 4 Static velostat® loading with 170 g

In attempt to analyze velostat® response to dynamic loading stepper motor was introduced. To simulate dynamic loading a stepper motor with pulley was fastened to bottom plate of testing device where velostat® is also fixed. Motor's pulley (Fig. 5) is designed with slots which allow to place weights in adjusting positions. Eccentric load combined with rotational movement acts as a vibrator dynamically loading velostat® in required frequency. By varying different weight size, its position and motor's rotational velocity different working conditions were simulated and further correlations analysed.

In dynamic testing bolt, nuts and washers acted as different size weights, m0 (without any weight), m1 (1 bolt, 2 washers and 2 nuts) – 2.2 g, m2 (1 bolt, 2 washers and 4 nuts) – 2.8 g and m3 (1 bolt, 2 washers and 6 nuts) – 3.4 g, which were placed in three positions shown in Fig. 5, P1 – 12 mm, P2 – 16 mm and P3 – 20 mm from pulley centre. To obtain relationship from loading frequency stepper motor angular velocity was configured according following values V1 – 4 rpm, v2 – 4.75 rpm, v3 – 5.5 rpm.

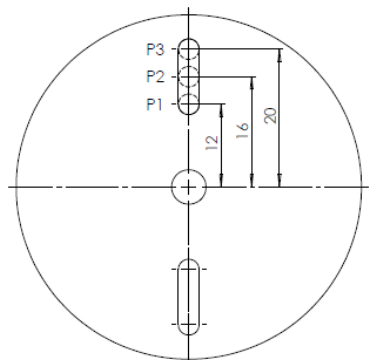


Fig. 5 Load positions on testing device pulley

Research results

In current chapter obtained research results are graphically represented by charts allowing to make further analysis and conclusions.

Fig. 6 represents data obtained from static velostat® loading. Dependency of resistance measured in Ohms to time is graphed while 6 different loads were applied. It is observed that resistance was growing from unloaded state till 100 g weight and then began to drop to initial state, resistances of m0 and m5 states are almost identical. As well it is noticeable that during constant loading values tend to grow or decay; m1, m2 and m4 are increasing their values, during m4 loading highest growth was marked with 0.86% from initial value; on the other hand m3 and m5 loading states were initially growing then reached their peak and begun to drop, although not falling lower their initial values.

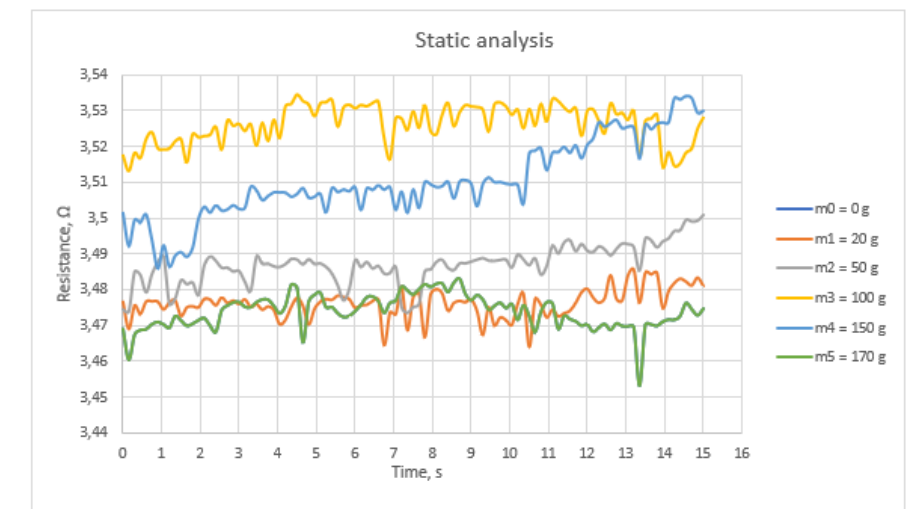


Fig. 1 Static analysis

Fig. 7 represents data obtained from dynamic velostat® loading regarding different mass variations. Dependency of resistance measured in Ohms to time is graphed while 4 different loads were applied in the same position and velocity. A clear dependency is noticed that with increasing mass velostat® tends to decrease its resistance also showing higher amplitude spikes because of inertia forces. Readings do not have any tendency to grow or decay showing good repeatability properties.

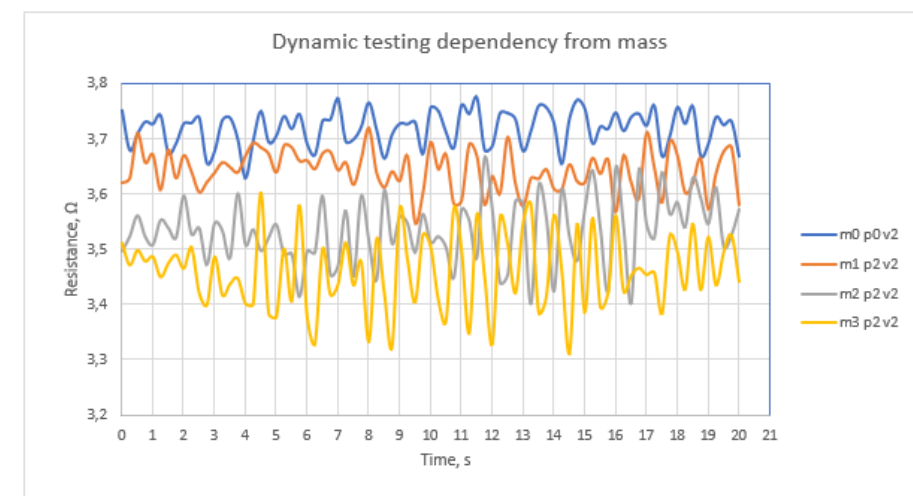


Fig. 2 Dynamic testing dependency from mass

Fig. 8 represents data obtained from dynamic velostat® loading regarding different load positioning variations. Dependency of resistance measured in Ohms to time is graphed while the same load is fixed in different positions under same velocity actuation. During operation in p3 position system experiences the highest mean resistance value, unexpectedly p1 outruns p2 in terms of mean resistance values. Because of constant velocity all fixture positions share the same wave frequency.

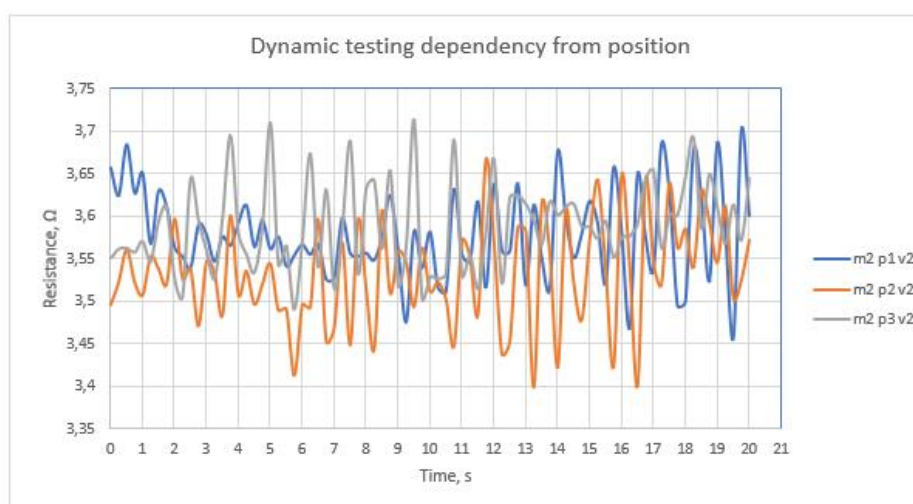


Fig. 3 Dynamic testing dependency from position

Fig. 9 represents data obtained from dynamic velostat® loading regarding different stepper motor velocity states. Dependency of resistance measured in Ohms to time is graphed while the same load is fixed in the one position but motor's angular velocity is altered. During v1 and v2 loading states sensor experiences rather similar reaction, although during v2 state after 11 seconds velostat® faces higher deviations in amplitude, as well as it was predicted system faces higher peaks in more frequent manner because of increase of velocity. During the highest velocity operation resistance value jumped up to 3.7 Ω in average experiencing lower amplitude spikes, although unexpected bigger distance between the peaks.

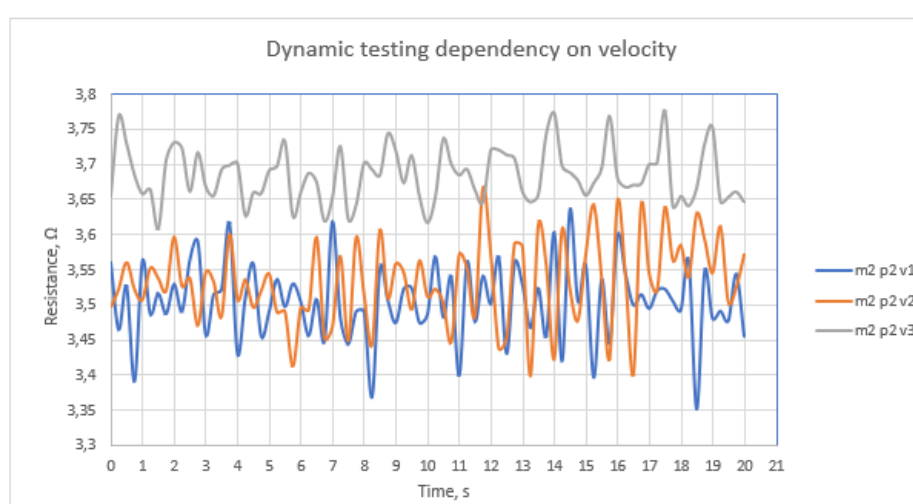


Fig. 4 Dynamic testing dependency from velocity

- [1] A. Dzedzickis, E. Sutins, V. Bucinskas, U. Samukaitė-Bubniene, B. Jakstys, A. Ramanavicius, I. Morkvenaitė-Vilkonciene, Polyethylene-Carbon Composite (Velostat®) Based Tactile Sensor, *Polymers* 2020, 12(12), 2905 (2020).
- [2] Zhang, Y.; Li, L. Modelling and design of MEMS piezoresistive out-of-plane shear and normal stress sensors. *Sensors* 2018, 18, 3737. [CrossRef] [PubMed]
- [3] Palmer, M.C.; O'Rourke, T.D.; Olson, N.A.; Abdoun, T.; Ha, D.; O'Rourke, M.J. Tactile pressure sensors for soil-structure interaction assessment. *J. Geotech. Geoenviron. Eng.* 2009, 135, 1638–1645. [CrossRef]
- [4] Wakabayashi, S.; Arie, T.; Akita, S.; Takei, K. Very thin, macroscale, flexible, tactile pressure sensor sheet. *ACS Omega* 2020, 5, 17721–17725. [CrossRef] [PubMed]
- [5] Li, J.; Chen, S.; Peng, Z.; Deng, Z.; Xing, S.; Wu, Y.; Liu, S.; Liu, L. A multidimensional hierarchical structure designed for lateral strain-isolated ultrasensitive pressure sensing. *J. Mater. Chem. C* 2020, 8, 922–929. [CrossRef]
- [6] Stassi, S.; Cauda, V.; Canavese, G.; Pirri, C.F. Flexible tactile sensing based on piezoresistive composites: A review. *Sensors* 2014, 14, 5296–5332. [CrossRef]
- [7] Yousef, H.; Boukallel, M.; Althoefer, K. Tactile sensing for dexterous in-hand manipulation in robotics—A review. *Sens. Actuators A Phys.* 2011, 167, 171–187. [CrossRef]
- [8] Zhang, Y.; Ye, J.; Lin, Z.; Huang, S.; Wang, H.; Wu, H. A piezoresistive tactile sensor for a large area employing neural network. *Sensors* 2018, 19, 27. [CrossRef]
- [9] Hopkins, M.; Vaidyanathan, R.; McGregor, A.H. Examination of the performance characteristics of velostat as an in-socket pressure sensor. *IEEE Sens. J.* 2020, 20, 6992–7000. [CrossRef]
- [10] Wen, F.; Sun, Z.; He, T.; Shi, Q.; Zhu, M.; Zhang, Z.; Li, L.; Zhang, T.; Lee, C. Machine learning glove using self-powered conductive superhydrophobic triboelectric textile for gesture recognition in VR/AR applications. *Adv. Sci.* 2020, 7, 2000261. [CrossRef]
- [11] <http://www.farnell.com/datasheets/1815591.pdf> - physical properties